Arun K. Ramanathan, Leon M. Headings, Marcelo J. Dapino, "Preliminary investigation of a differential pressure sensor using flexible piezoelectrics with pyroelectric compensation," Proc. SPIE 11382, Smart Structures and NDE for Industry 4.0, Smart Cities, and Energy Systems, 113820I (20 May 2020); https://doi.org/10.1117/12.2558725

Preliminary investigation of a differential pressure sensor using flexible piezoelectrics with pyroelectric compensation

Arun K. Ramanathan, Leon M. Headings, and Marcelo J. Dapino*

NSF IUCRC on Smart Vehicle Concepts, Department of Mechanical and Aerospace Engineering, The Ohio State University, Columbus, OH 43210

ABSTRACT

Pressure sensors that can provide both high temporal and spatial resolutions are desired for the measurement of aerodynamic and acoustic events, ultrasonics, and underwater phenomena. Piezoelectric materials are attractive candidates for measuring dynamic pressure due to their high sensitivity, high signal-to-noise ratio, and potential for miniaturization. However, their inability to directly measure static pressure prevents their use in many applications. Due to their strong pyroelectric response, their use is also generally limited to conditions where the rate of temperature change is below the lower cutoff frequency of the measurement system. Polyvinylidene fluoride (PVDF) is a polymer with a high piezoelectric sensitivity which is readily available as a flexible, tough film. Under steady flow conditions, configuring PVDF as a cantilever unimorph provides a higher pressure sensitivity than alternatives such as compressive, doubly clamped, or diaphragm configurations. In this work, we demonstrate a differential aerodynamic pressure sensor based on a cantilever PVDF unimorph that has been optimized to maximize pressure sensitivity for a targeted deflection sensitivity. The sensor is characterized using a laboratory-scale wind tunnel for flows ranging from 0 to 12 m s^{-1}. Near-static measurements are enabled by a compensated charge amplifier with an extremely low cutoff frequency. The pyroelectric voltage generated from changes in the air flow temperature is compensated using a PVDF sensor in compressive mode. Within the tested pressure range of 0 to 80 Pa, the sensor exhibits a proportional response with a sensitivity of 0.97 mV Pa^{-1}.

Keywords: differential pressure sensor, flexible, piezoelectric, pyroelectric, wind tunnel measurements

1. INTRODUCTION

Automotive aerodynamic measurements require pressure transducers that can simultaneously provide both high temporal and spatial resolutions.[1,2] Commercial piezoresistive pressure transducers possess low sensitivity, require external power, and are susceptible to electrical noise. Piezoelectric materials, on the other hand, possess the advantages of direct electromechanical conversion, high sensitivity, and superior noise immunity due to their capacitive nature. Further, the signal conditioners associated with piezoelectric sensors are smaller in construction and typically consume low external power.[3]

Flexible piezoelectric polymers such as polyvinylidene fluoride (PVDF) are promising alternatives to conventional pressure sensors due to their high compliance, low density, and ease of installation. Available as a thin film, PVDF is conformable and conducive to miniaturization for real-time flow measurements. Piezoelectric sensors generate charge due to stresses applied in compression (d_{33} mode)[4–6] and bending (d_{31} mode).[7,8] Most of the literature on piezoelectric films in ambient wind conditions focuses on unsteady and impulsive flow measurements. To accommodate an increased time constant for steady flow measurements, both compressive mode and diaphragm configurations require a considerable increase in the size of the sensor. It has been shown that the charge sensitivity of an optimized cantilever unimorph is three times higher than that of a doubly clamped unimorph with an optimized electrode coverage and three orders of magnitude greater than that of a compressive (d_{33} mode) sensor for the same sensor size.[9]

*Further author information: (Send correspondence to M.J.D.)
A.K.R.: E-mail: ramanathan.38@osu.edu
L.M.H.: E-mail: headings.4@osu.com
M.J.D.: E-mail: dapino.1@osu.edu

In addition to generating charge in response to an applied pressure, piezoelectric materials also generate charge in response to temperature changes (pyroelectricity). The pyroelectric response results from the temperature dependence of polarization which produces an electric charge on the PVDF surface. The total charge displacement of a PVDF sensor is equal to the sum of the piezoelectric and pyroelectric charge displacements.[10] By nature, wind possesses both pressure and temperature components. Due to the large pyroelectric constant for PVDF ($p = 30\ \mu\text{C m}^{-2}\ \text{K}^{-1}$), compensation techniques are required to isolate the piezoelectric component in the measured sensor voltage for pressure sensing. The low pressure sensitivity of a PVDF compressive sensor can be exploited to compensate for the pyroelectric effect of a cantilever PVDF sensor.

The objective of this article is to present a static differential pressure measurement system consisting of a cantilever PVDF sensor interfaced with a large time constant compensated charge amplifier. The pyroelectric response is compensated using a second PVDF sensor operating in compressive (d_{33}) mode. The design process to maximize the charge sensitivity of a PVDF unimorph for a given deflection sensitivity is presented in Section 2, along with the sensor fabrication procedure. In section 3, the sensor design is evaluated through the experimental characterization of a PVDF sensor with the proposed circuit topology and pyroelectric compensation strategy. The sensor presented is expected to serve as a piezoelectric alternative to conformable soft pressure sensing mats that can be integrated with arbitrarily-shaped structures for aerodynamic pressure measurements.

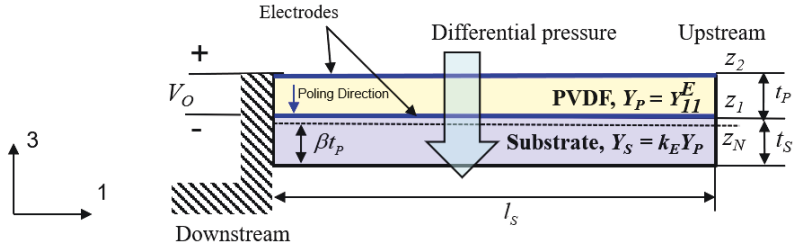

Figure 1: Schematic diagram of a piezoelectric unimorph cantilever sensor subjected to a uniform differential pressure showing: the thicknesses of the PVDF layer t_P and the substrate t_S, elastic moduli along direction 1 for the PVDF layer under constant electric field Y_P and the substrate Y_S, unimorph length l_S and width b_S, and distance between the bottom of the substrate and the neutral axis of the structure βt_P.

2. DESIGN AND FABRICATION OF PIEZOELECTRIC CANTILEVER SENSOR

2.1 Design optimization procedure

The configuration of a PVDF unimorph beam is shown in Figure 1. The structure has an overall length of l_S and width of b_S. The elastic modulus of the substrate is Y_S and, at constant electric field, the elastic modulus in direction 1 for the PVDF layer is Y_P, with an elastic modulus ratio defined as $k_E = Y_S/Y_P$. The thicknesses of the PVDF layer and the substrate are t_P and t_S, respectively, with a thickness ratio defined as $k_t = t_S/t_P$. It is assumed that longitudinal stress T_1 is the primary source of charge generated by the PVDF layer. The charge generated by the lateral stress T_2 can be neglected because lateral stress is much smaller than longitudinal stress in unimorph bending and also because the piezoelectric piezoelectric strain constant d_{32} is much smaller than d_{31}.[11]

Using classical laminate theory and Euler-Bernouilli conditions for a cantilever unimorph, the charge sensitivity Q_P is defined as charge generated Q per unit applied pressure P and the deflection sensitivity δ_P is defined as maximum deflection w_{max} per unit applied pressure P:[12]

$$\begin{aligned} Q_P &= \frac{Q}{P} = -\frac{0.167 d_{31} b_S^2 Y_P t_P l_S^3}{\overline{YI}}(0.5 + k_t + \beta) \text{ and} \\ \delta_P &= \frac{w_{max}}{P} = \frac{b_S l_S^4}{8\overline{YI}}, \end{aligned} \tag{1}$$

Table 1: Geometric and material properties of the PVDF unimorph pressure sensor.

Geometric parameters of the sensor		Material properties of the PVDF film	
Length x width of the cantilever l_S x w_S	10 x 10 [mm^2]	Elastic modulus, Y_P	2.74 [GPa]
Thickness of PLA substrate	0.196 [mm]	Relative permittivity, ϵ_r	11-13
Thickness of PVDF film, t_P	28 [μm]	Piezoelectric charge coefficient in direction 1, d_{31}	24 [pC N^{-1}]
Overall length of the sensor	22 [mm]	Piezoelectric charge coefficient in direction 2, d_{32}	3 [pC N^{-1}]
Overall width of the sensor	12 [mm]	Piezoelectric charge coefficient in direction 3, d_{33}	-34 [pC N^{-1}]
Overall thickness of the sensor	1.23 [mm]	Pyroelectric coefficient, p	30 [μC m^{-2} ^{o}C^{-1}]

where

$$\overline{YI} = \frac{Y_P b t_P^3}{3}\left[k_E k_t\left(k_t^2 + 3\beta k_t + 3\beta^2\right) + \frac{1}{1-k_{31}^2}\left\{\left(1 - \frac{3k_{31}^2}{4}\right) + 3\left(1-k_{31}^2\right)\left(k_t^2 + \beta^2 + 2\beta k_t + k_t + \beta\right)\right\}\right]$$

is the bending stiffness of the unimorph.

For overall thickness and pressure limit targets of 1 mm and 2 kPa, respectively, the targeted deflection sensitivity δ_P is calculated to be 0.5 μm/Pa. The thickness ratio k_t is investigated over the range of 2 to 20 and the elastic modulus ratio k_E is investigated from 0.1 to 70. The optimal elastic modulus ratio and the optimal thickness ratio to maximize charge sensitivity $Q_{P,max}$ are calculated to be 0.2 and 7, respectively.[12] In order to use a commercial 3D printer for rapid prototyping of the substrate, polylactic acid (PLA) with $k_E = 0.73$ is selected as the feedstock with an elastic modulus ratio closest to the optimal. Table 1 lists the geometric and material properties for the PVDF unimorph pressure sensor design. A detailed account of the analytical model and the design optimization procedure is provided in Ramanathan et al.[12]

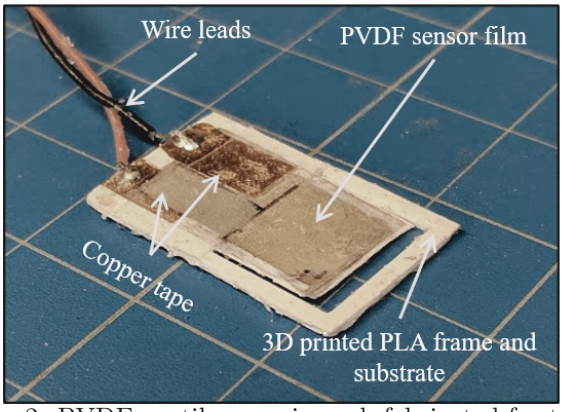

Figure 2: PVDF cantilever unimorph fabricated for testing.

2.2 Fabrication process

The sensor frame and the substrate of the cantilever unimorph are 3D printed as a single part using a commercial printer (Ultimaker S5). Polylactic acid (PLA) is printed at 190°C with a print speed of 25 mm/s and a 100% infill diagonal raster. The PVDF is cut to a length of 17.0 mm and width of 10.5 mm from a 28 μm thick commercial PVDF film with sputtered silver electrodes (Measurement Specialties). Leads for the electrodes are created by attaching 10 mm x 3 mm copper tapes with conductive adhesive. To strengthen the attachments between the PVDF and copper tapes, a thin coating of acrylic is applied to both sides and allowed to cure for 24 hours at room temperature. Next, the PVDF film with attached leads is bonded to the 3D printed part with

a thin layer of cyanoacrylate glue (3M) and clamped for 30 minutes during curing. The sensor is completed by soldering wire leads onto the copper tape, yielding the sensor shown in Figure 2. Table 1 provides the overall dimensions of the physical sensor.

3. EXPERIMENTAL CHARACTERIZATION

3.1 Signal conditioner for near static measurements

A basic charge amplifier can be constructed from an operational amplifier and discrete electronic components. This type of amplifier typically has characteristics of a band-pass filter with a time constant that results from by the sensor impedance and the feedback impedance. While the circuit can be designed to provide a large time constant, basic charge amplifiers are sensitive to input bias currents I_{B-} and I_{B+}, which cause error to accumulate from drifting of the output voltage. A detailed analysis of the effect of circuit parameters on drift error as well as a differential charge amplifier design to overcome this limitation are provided in our previous work.[13] A compact version of the differential charge amplifier is utilized in this work. The insulating resistances of the capacitors extend the time constant of the system up to 10^5 seconds. Assuming $C_F = C_C$ and $R_F = R_C$ for the compensated charge amplifier shown in Figure 3, the output voltage in the Laplace domain $V_M(s)$ for a step charge input is given by

$$V_M(s) = \left(\frac{2S_Q}{s + f_{LC}}\right) sQ(s) + \left\{\frac{S_Q I_{B-}}{s + f_{LC}}\,(1 - t_B)\right\}, \tag{2}$$

where S_Q corresponds to the single-ended voltage gain of the charge amplifier, f_{LC} corresponds to its lower cutoff frequency, and $t_B = I_{B+}/I_{B-}$. The differential charge amplifier configuration produces a passband gain S_Q that is twice that of a basic single-ended configuration. Variations due to component tolerances for capacitances C_F and input bias currents I_{B-} and I_{B+} become significant as the cutoff frequency approaches zero, leading to error in long time static measurements. Therefore, in order to minimize the drift rate, capacitors C_F and C_C should be matched as closely as possible (with leakage resistance $R_F > 1$ TΩ) and operational amplifiers should be selected that have low bias currents (< 0.1 pA) and high open loop gain (> 100 dB). The design parameters for the signal conditioner circuit are shown in Table 2.

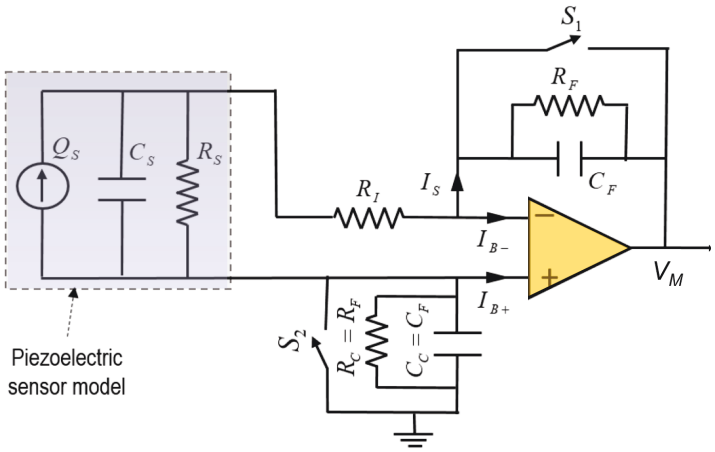

Figure 3: Schematic of the compensated charge amplifier for near static measurements.

3.2 Experimental setup

The piezoelectric differential pressure sensor is tested under different aerodynamic pressures using a wind tunnel (Pitsco X-Stream). The wind tunnel has test chamber dimensions of 500 mm x 300 mm x 300 mm and a flow straightener for flow laminarization and low flow restriction. It produces a controllable flow velocity up to 15 m/s, which is measured using a manometer.

Table 2: Circuit parameters utilized for the construction of the signal conditioner.

Parameter	Value
Op-amp type	LMC 6082
$C_F = C_C$	10 nF ± 1%
C_S	0.65 nF
R_I	1 MΩ
I_B	0.1 pA max.
Time constant	$\sim 10^5$ seconds
Insulating resistances	$\sim$ 100 GΩ

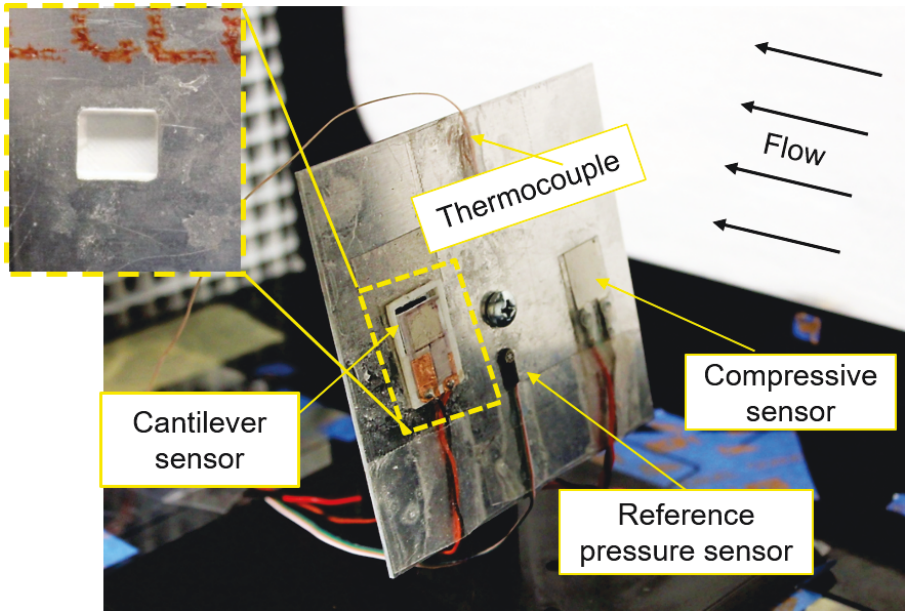

Figure 4: Wind tunnel test setup for characterizing the PVDF pressure sensor. Pressure is measured on a flat plate with a square cutout to accommodate the PVDF differential pressure sensor. The compressive mode PVDF sensor for pyrolectric compensation is placed symmetrically on the other half of the plate. A reference piezoresistive pressure sensor and a thermocouple are also mounted to measure the aerodynamic pressure and temperature. The inset shows the machined cutout from the back side of the plate.

The experimental setup in the wind tunnel is shown in Figure 4. The PVDF pressure sensor is tested on a flat plate that is held in a sloped position using a 3D printed fixture. The 100 mm x 100 mm aluminum plate has a 12 mm x 12 mm square cutout to accommodate the PVDF differential pressure sensor. The sensor, shown in Figure 2, is attached at the square cutout using double-sided tape. To provide pyroelectric compensation, a 10 mm x 10 mm compressive-mode PVDF sensor is attached with cyanoacrylate adhesive at a symmetric location on the other half of the plate. A commercial piezoresistive pressure sensor (Kulite LQ-062) with a sensing range of 0 to 35 kPa and a full scale output of 100 mV is also attached to the plate to measure the applied pressure.[14] Airflow temperature at the plate is measured with a thermocouple (Omega Engineering AWG40 wire). All measurements are recorded at a sampling rate of 10 Hz with a data acquisition system (NI 9239).

The experimental procedure is to turn the wind tunnel off for 50 seconds before switching it on for the next 200 seconds. The flow rate is measured using the wind tunnel's manometer and the applied differential pressure is measured using the reference pressure sensor. Due to the low sensitivity of the reference sensor, a 50-point Gaussian average is used to smooth the signal and the average pressure is taken as the measured reference pressure at that flow rate. The flow is turned off after 200 seconds and the next set of measurements are taken only after the temperature stabilizes within the test chamber. The signal conditioners for the reference pressure sensor and the PVDF sensor are reset before the start of the next set of measurements.

3.3 Results and discussion

The responses of the cantilever and compressive PVDF sensors with compensated charge amplifiers are shown for two different pressures in Figure 5 (a) and (b). Thermocouple measurements show that the temperature decreased as much as 0.8 °C during the wind tunnel tests. The cantilever and compressive sensors exhibit similar transient responses to the temperature input. The temperature change measured by the thermocouple is plotted on the

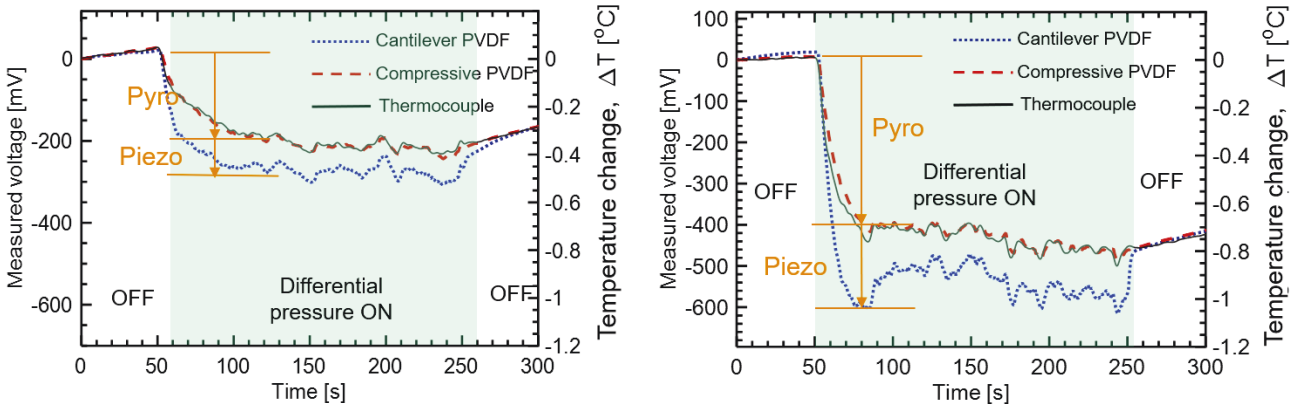

Figure 5: Comparison of the thermocouple response and the responses of the cantilever and compressive PVDF sensors interfaced with the compensated charge amplifier at (a) low pressure, $P = 23$ Pa, and (b) high pressure, $P = 85$ Pa. The initial temperature was measured to be 26.8 °C.

secondary y-axis, which is scaled based on the calculated pyroelectric sensitivity of $pA_S\Delta T = 570$ mV °C^{-1}. The long sample period of the measurement and the corresponding voltage responses of the sensors demonstrate the near static measurement capability of the sensing system. The cantilever sensor responds slightly faster than the compressive sensor to the change in temperature due to its lower thermal capacitance. It is also observed from the arrows in Figure 5 that the average difference between the cantilever and the compressive sensor voltages is higher for a higher applied pressure P. When the flow is turned off, the magnitude of the cantilever sensor voltage (V_A) quickly decreases to the voltage of the compressive sensor (V_D), which shows that the differential voltage ($V_D - V_A$) is caused by the piezoelectric contribution (V_P) to the voltage output. Over the ranges investigated, no direct relationships are observed between the change in temperature, effective pyroelectric sensitivities of the sensors, and flow rate.

The compensated voltage responses of the PVDF sensor are shown in Figure 6(a) for different flow rates. A positive correlation is observed between flow rate and compensated voltage at the instant the flow is turned on, but the signals do not stabilize until about 60 seconds later. It is hypothesized that this is due to the difference in thermal characteristics between the cantilever sensor and the compensation sensor as well as temperature variation in the wind tunnel. Furthermore, it is observed that the compensated voltage does not immediately return to zero when the flow is turned off. Therefore, a pyroelectric compensation algorithm or a pyroelectric compensation sensor with thermal characteristics that match the cantilever unimorph sensor is required to eliminate the residual pyroelectric component in the compensated voltage. The average compensated voltage is calculated after the voltage reaches steady state. Figure 6(b) shows the mean compensated voltage against measured reference pressure. The sensor exhibits good proportionality and the measured sensitivity of 0.97 mV Pa^{-1} is very close to the theoretical model sensitivity of 0.99 mV Pa^{-1}.

4. CONCLUDING REMARKS

A novel sensing system for steady differential pressure measurement is demonstrated using a cantilever PVDF unimorph. Deflection and charge sensitivities for a PVDF cantilever unimorph under a uniform applied pressure are calculated from generalized expressions for the deflection and polarization of piezoelectric bending unimorphs.

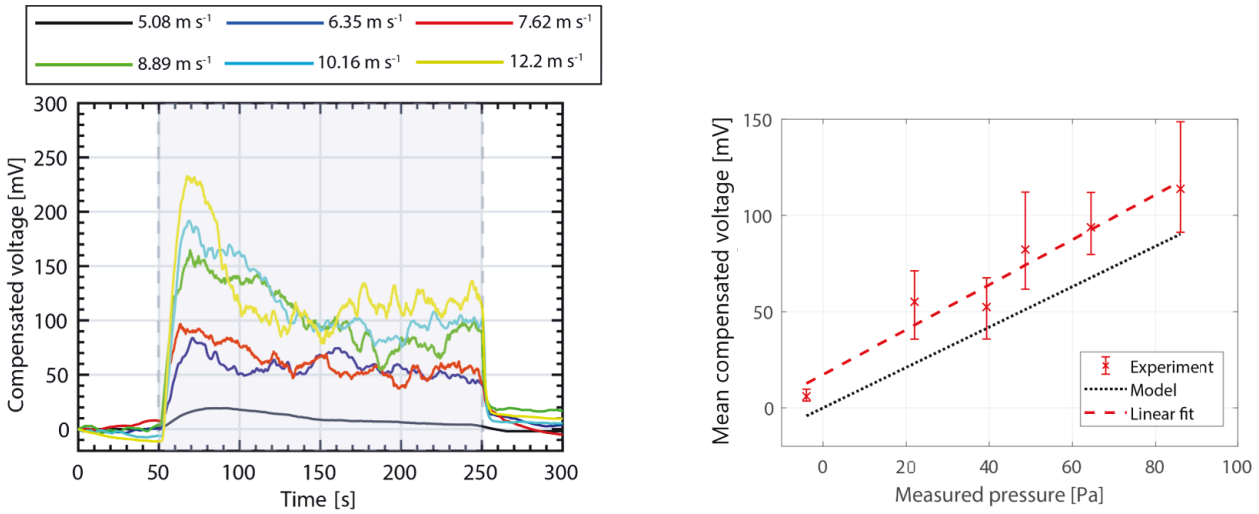

(a) (b)

Figure 6: (a) Compensated voltage ($V_D - V_A$) response for different input flow rates. (b) Average compensated voltage versus measured reference pressure for comparison of the experimental (with linear fit) and theoretical (modeled) sensitivities, represented by the slopes.

Taking material availability and ease of fabrication into consideration, a 0.2 mm thick PLA polymer is chosen as the substrate and fabricated using a commercial FDM printer in order to meet the deflection sensitivity target while maximizing charge sensitivity. Near-static measurement is enabled via an automated drift compensation circuit constructed from discrete components. The sensor is fabricated and experimentally characterized over a pressure range of 0 to 80 Pa using a laboratory wind tunnel. The pyroelectric noise due to temperature change is compensated with a compressive mode pressure sensor interfaced with another compensated charge amplifier. The primary advantage of this pyroelectric compensation technique over thermocouple-based techniques is that the compensation sensor operates on the same measurement principle as the pressure sensor, which minimizes noise contamination in the compensated voltage. Also, it may be possible to package the compensator within the cantilever structure via MEMS techniques. The sensor exhibits good proportionality with a sensitivity 0.97 mV Pa^{-1}, which is close to the calculated theoretical model sensitivity of 0.99 mV Pa^{-1}. Large variations in the compensated voltage are primarily due to residual error after pyroelectric compensation, thus warranting a realtime compensation sensor with thermal characteristics better matching the pressure sensor in order to further reduce the error. One method to achieve matched transient thermal response is to integrate the pyroelectric compensation sensor onto the cantilever sensor. Finally, the differential pressure measurement technique will be extended towards the development of a conformable piezoelectric absolute wind pressure sensor mat.

Acknowledgements

Financial support was provided by the member organizations of the Smart Vehicle Concepts Center, a Phase III National Science Foundation Industry-University Cooperative Research Center (www.SmartVehicleCenter.org) under grant NSF IIP 1738723.

REFERENCES

[1] T. Stathopoulos, I. Zisis, and E. Xypnitou, "Local and overall wind pressure and force coefficients for solar panels," *Journal of Wind Engineering and Industrial Aerodynamics* **125**, pp. 195–206, 2014.

[2] T. Yamashita, T. Makihara, K. Maeda, and K. Tadakuma, "Unsteady aerodynamic response of a vehicle by natural wind generator of a full-scale wind tunnel," *SAE International Journal of Passenger Cars-Mechanical Systems* **10**(2017-01-1549), pp. 358–368, 2017.

[3] I. Mahbub, S. Shamsir, S. K. Islam, S. A. Pullano, and A. S. Fiorillo, "A low noise front-end amplifier for pyroelectric transducer based respiration monitoring system," in *2017 IEEE 60th International Midwest Symposium on Circuits and Systems (MWSCAS)*, pp. 875–878, Aug 2017.

[4] W. Nitsche, P. Mirow, and J. Szodruch, "Piezo-electric foils as a means of sensing unsteady surface forces," *Experiments in Fluids* **7**(2), pp. 111–118, 1989.

[5] W. Luber and J. Becker, "Application of PVDF foils for the measurements of unsteady pressures on wind tunnel models for the prediction of aircraft vibrations," in *Structural Dynamics, Volume 3*, pp. 1157–1176, Springer, 2011.

[6] Y. Wang, C. Huang, Y. Lee, and H. Tsai, "Development of a PVDF sensor array for measurement of the impulsive pressure generated by cavitation bubble collapse," *Experiments in Fluids* **41**(3), pp. 365–373, 2006.

[7] M. Niu and E. Kim, "Piezoelectric bimorph microphone built on micromachined parylene diaphragm," *Journal of Microelectromechanical Systems* **12**(6), pp. 892–898, 2003.

[8] H. Takahashi, A. Isozaki, K. Matsumoto, and I. Shimoyama, "A cantilever with comb structure modeled by a bristled wing of thrips for slight air leak," in *2015 28th IEEE International Conference on Micro Electro Mechanical Systems (MEMS)*, pp. 706–709, IEEE, 2015.

[9] A. Ramanathan, L. Headings, and M. Dapino, "Design optimization of flexible piezoelectric PVDF unimorphs for surface pressure transducer applications," in *Smart Structures and NDE for Energy Systems and Industry 4.0*, **10973**, p. 1097307, International Society for Optics and Photonics, 2019.

[10] A. Khan, Z. Abas, H. Kim, and I. Oh, "Piezoelectric thin films: an integrated review of transducers and energy harvesting," *Smart Materials and Structures* **25**(5), p. 053002, 2016.

[11] Measurement Specialties, Inc., *Piezo Film Sensors Technical Manual*, 1999.

[12] A. K. Ramanathan, L. M. Headings, and M. J. Dapino, "Differential pressure sensor using flexible piezoelectrics with pyroelectric compensation," *In preparation* .

[13] A. K. Ramanathan, L. M. Headings, and M. J. Dapino, "Near static strain measurement with piezoelectric films," *Sensors and Actuators A: Physical* **301**, p. 111654, 2020.

[14] Kulite Semiconductor Products, *Kulite strain gage manual*, 2012.